

# HYDROCARBON FUEL BASED ON BALL-MILLED ALUMINIUM AND DODECANE

*Florian Chantre\*<sup>†</sup>, Marc Bouchez\*<sup>†</sup>, Olivier Poncelet\*\**

*\* MBDA France : Rondpoint Marcel Hanriot, Route d'Issoudun, 18020 Bourges*

*\*\* CEA Tech : 17 Rue des Martyrs, 38000 Grenoble*

florian.chantre@mbda-systems.com marc.bouchez@mbda-systems.com

<sup>†</sup> Corresponding Authors

**Keywords:** fuel / airbreathing propulsion / ramjet / nanoparticles / aluminium / dodecane / performances / nanotechnologies

## Abstract

Nano-fluids are more and more studied in numerous industry areas (medical, energetic, nuclear...). They have particular flow properties and many corresponding models are available. Particularly, the use of nano-fuels (liquid fuels with particles of less than 100 nanometers typically) is moving more and more from laboratory to advanced studies for automotive (a few percent of nanoparticles) and aerospace (several dozen percent of nanoparticles) applications.

MBDA identified in 2015 the possible interest of nanotechnologies and associated possible game-changers or at least techno-enablers, and carried out a free survey in connection with several of its research partners like ENSTA, CNRS, CEA, and ONERA. The interest of nanoparticles to fuel is not new and had been investigated in the past, especially with the “slurry fuels” studied extensively at the end of the last century.

The current trend is to use a smaller amount of quite smaller particles, and estimate the possible operational benefit for future systems as well as the associated showstoppers or risk mitigation actions.

For example, a theoretical work was awarded by MBDA at ENSTA lab in Paris in order to assess by detailed kinetic modelling what could be the benefit (or the lack of performance) of small particles add-on, for combustion range (ignition, blow-off...). This work does not take into account the liquid state of the fuel as well as the size and geometry of metallic particles, but it allowed to state how the fuel ignition delay is modified, for instance by aluminium.

Existing (and scattered) models were used to predict what could be the combustion heating value, the density and, with less accuracy, the expected viscosity and thermal conductivity evolutions with temperature.

Propulsion but also cooling performance could be increased by 20 to 40% compared to base fuel without nanoparticles, but many limitation factors have to be taken into account. Risks for safety, security and handling have been assessed. The Research & Technology activity reported here is then dealing with the use of nanofuels for aerospace applications, especially for future airbreathing systems, including in a “drop-in” option.

Current aviation fuels like kerosene are formed of hundreds or thousands of chemical species, thus they are not easy to manage computationally in an R&T study like in the current prospective activity conducted by MBDA and CEA on ‘nanofuels’.

N-dodecane ( $n\text{-C}_{12}\text{H}_{26}$ ) has been chosen as a basis generic fuel since this alkane hydrocarbon could have a quite similar overall behaviour in engines as regular kerosene. Laboratory tests of dodecane mixed with aluminium nano-sized particles were conducted and analysed, some results will be discussed here, and compared to theoretical or system computations.

## 1. Introduction

Nanofluids are more and more studied in numerous business areas (medical, energetic, nuclear...). They have particular flow properties and many corresponding models are available. Particularly, use of nano-fuels (“NF”: liquid fuels with particles of less than 100 nanometers) is moving more and more from laboratory to advanced studies for automotive (a few percent of nanoparticles) and aerospace (some tens of nanoparticles) applications [1][2][3]. MBDA had identified in 2015 the possible interest of nanotechnologies and associated possible game-changers or at least techno-

enablers, and did a free survey in connexion with several of its research partners like ENSTA, CNRS, CEA, and ONERA. The interest of nanoparticles to fuel is not new and was investigated in the past, especially with the “slurry fuels” studied extensively at the end of last century, including in France by ONERA and MBDA [4]

The current trend is to use a smaller amount of quite smaller particles, and estimate the possible operational benefit for future systems as well as the associated showstoppers or risk mitigation actions. For example, a theoretical work was awarded by MBDA at ENSTA lab in Paris in order to assess by detailed kinetic modelling what could be the benefit (or the lack of performance) of small particles, for combustion range (ignition, blow-off, ...). This work does not take into account the liquid state of the fuel as well as the size and architecture of metallic particles but it allowed to state how the fuel ignition delay should be better with pure aluminium Al addition or, at the opposite, increased in the vicinity of alumina  $\text{Al}_2\text{O}_3$  [5]

Existing (and scattered) models were used to predict what could be the combustion heating value, the density and, with less accuracy, the expected viscosity and thermal conductivity evolution with temperature.

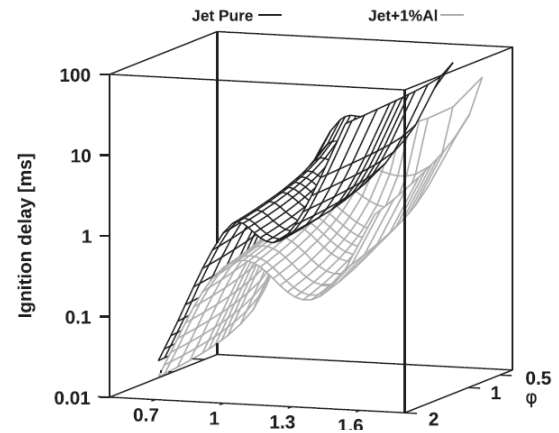


Figure 1 : Ignition delay variation as a function of initial temperatures and equivalence ratios, as published in [5]

In the meantime, some actual (even if subscale) test of engines have been publically reported where nanofuels confirmed their theoretical power. For example, rocket engine tests were published in [6] a few years ago, with a dense fuel with or without about 16% of aluminium nanoparticles (Alex), showing by measurements an increase of combustion efficiency, thrust and even specific impulse (this last point was not expected by theoretical computations).

For airbreathing systems, another team published in 2021 such kind of experimental results in a supersonic combustion ramjet [7]. This study confirmed experimentally both the benefit for combustion efficiency derived from measured wall pressure increase as well as the Equivalence Ratio (ER) range with the same kind of nanofuels (+16 wt% Alex). In this example, for an Equivalence Ratio of 0.56, this team showed a performance benefit of 16% for the specific impulse, more or less proportional to expected range in cruise, unexpectedly leading to a volumetric specific impulse increase of 35% that would hence increase the Specific Impulse (ISP) benefit.

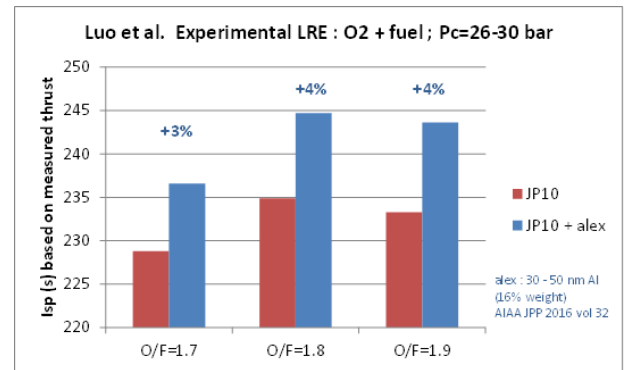


Figure 3 : Liquid Rocket performance benefit with nanofuel, as published in [6]

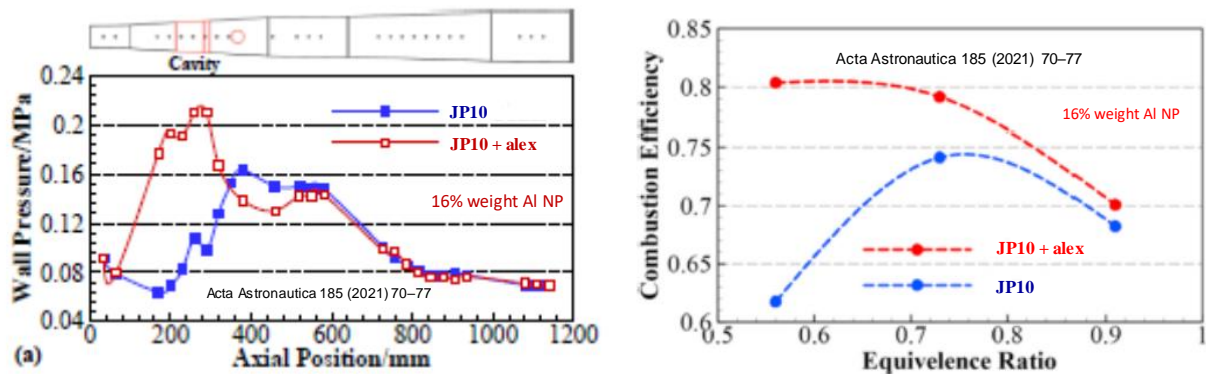


Figure 2: Supersonic combustion benefit with Nanofuels, as published in [7]

Using other fuels (here JP-10 and QuadriCyclane) and particles more energetic than aluminium could obviously lead to higher benefit. For example, the results in [8] show than a volumetric heating value of 53MJ/litter to be compared with 40 MJ/litter for regular fuels.

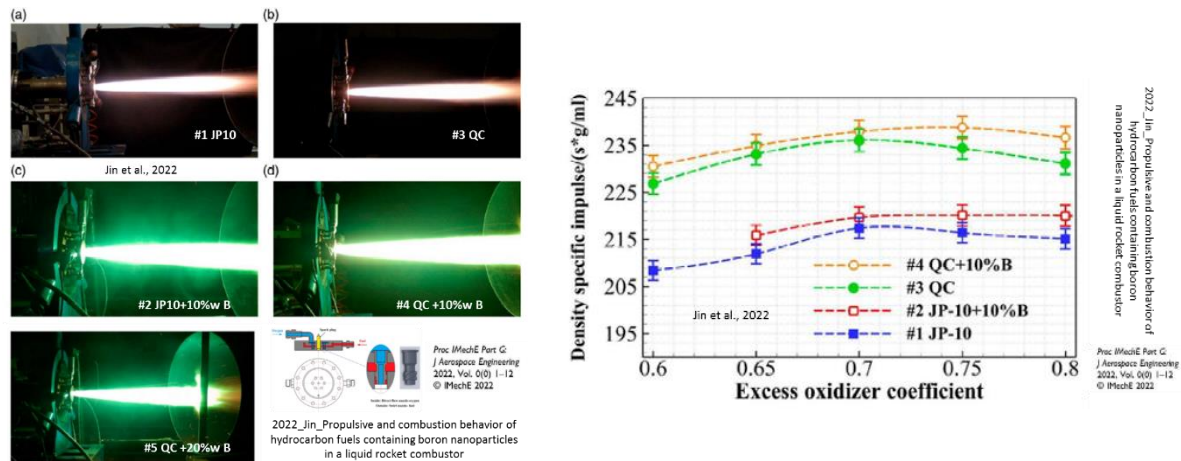


Figure 4 : Literature test of energetic nanofuels investigated in existing liquid rocket engine, as published in [8]

Propulsion but also cooling performance could be increased by 20 to 40% compared to base fuel without nanoparticles, but many limitation factors have to be taken into account.

Risks for safety, security and handling have been assessed in the current study by CEA with MBDA and other partners. The present activity is then dealing with the use of nanofuels for aerospace applications, especially for future air breathing systems, including in a “drop-in” option.

Kerosene does not have a clearly determined composition, as this petrochemical product is defined only by its required properties (with some margin). Moreover, current fuels like kerosene are formed of hundreds or thousands of chemical species, thus they are not easy to manage computationally in an R&T study like in the current prospective activity conducted by MBDA and CEA on ‘nanofuels’.

N-Dodecane (n-C12) is a surrogate fuel of actual fuels like kerosene’s (TR0, jet-A...). To replicate the overall behaviour of actual kerosene fuels, especially in combustion, it should be associated with other components. Several test series have shown that n-C12 can have the same overall behaviour in engines as regular kerosene. For instance, series of tests in the USAF referee combustor AFRL [9] show similar combustion efficiency and fuel temperature effect with jet-A (A-2 below) and n-C12 in Figure 5.

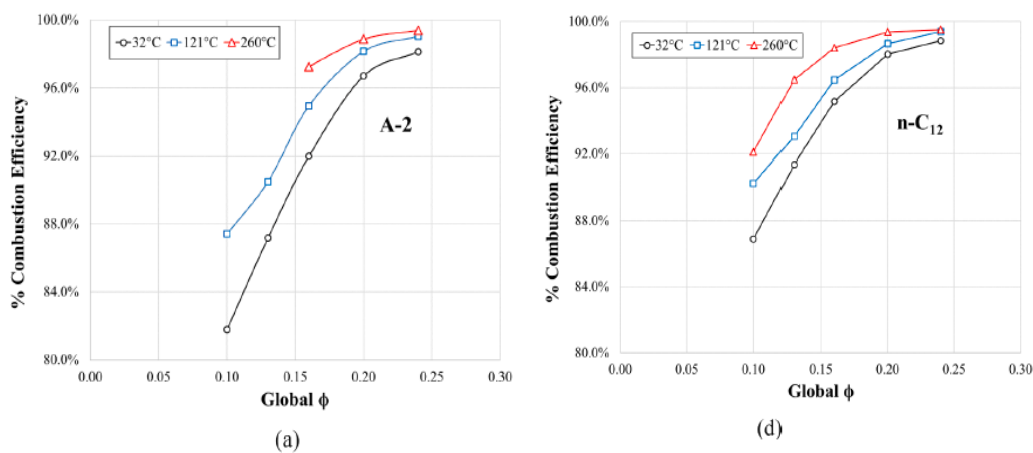


Figure 5: Comparison of combustion efficiency of kerosene (left) and n-C12 (right) in the AFRL referee combustor test in [9]

Therefore, n-dodecane was chosen as a good « academic fuel » for the current assessment of nanofuel behaviour. In terms of properties, n-dodecane is quite different to a Jet-A fuel. The choice of n-C12 is also a way to diversify fuels that we use in Research and Technology, in anticipation of the “fuel revolution” in following years (bio fuels for instance).

Aluminium has many advantages for an academic study. It is easy to obtain at different sizes and shape of particles and is also well documented (kinetic and energetic modelling). Therefore, aluminium is used as add-on for the exploratory study by MBDA and CEA. Table 1 recalls the typical energetic and density characteristics of the different fuels considered in the present study.

Material	LHV <sub>m</sub> (MJ/kg)	$\rho$ (kg/L)	LHV <sub>v</sub> (MJ/L)	$\Delta$ LHV <sub>v</sub> in relation to n-C12
Aluminium	31.00	2.70	83.70	-
Dodecane (n-C12)	44.68	0.749	33.47	-
Kerosene Jet-A	43.15	0.8	34.5	+3.1 %
n-C12 + 5 wt% Al	44.00 <sup>1</sup>	0.777 <sup>1</sup>	34.19 <sup>1</sup>	+2.2 % <sup>1</sup>
n-C12 + 10 wt% Al	43.31 <sup>1</sup>	0.807 <sup>1</sup>	34.97 <sup>1</sup>	+4.5 % <sup>1</sup>
n-C12 + 15 wt% Al	42.63 <sup>1</sup>	0.840 <sup>1</sup>	35.81 <sup>1</sup>	+7.0 % <sup>1</sup>
n-C12 + 20 wt% Al	41.94 <sup>1</sup>	0.876 <sup>1</sup>	36.72 <sup>1</sup>	+9.7 % <sup>1</sup>

<sup>1</sup> - Theoretical values of LHV and density

Table 1: Density and calculated heats of combustion of different materials

## 2. Experimental

Commercial aluminium powder were ball-milled with n-dodecane to produce the metallized fuel. The density measurements were carried out with the help of an apparatus DMA 4100 M. The specific surface area (SSA) was measured by the method of Brunauer-Emmett-Teller (BET) using a BELSORP-max apparatus. The XRD analysis was carried out with a D8 Bruker diffractometer using Cu-K $\alpha$  radiation. The aluminium and aluminium oxide contents in the oxidised products were determined from XRD analysis data using the RIR (relative intensity ratio) method and the software DIFFRAC.EVA v.5.2. SEM images were obtained with the help of a Hitachi 4000 microscope. The TG-DSC (thermogravimetric - differential scanning calorimetry) analysis was carried out using an apparatus Setaram Lab Sys Evo 1600 in an airflow of 20 ml/min from 30 to 1200°C with a heating rate of 10 K/min. The values of the combustion heat (also called *heating values* or *calorific values*) were experimentally determined using a bomb calorimeter Parr 6100. The combustion heating values indicated below are lower ones (LHV) as they were obtained after subtracting the energy related to the vaporisation of water.

## 3. Results and discussion

### 3.1. Characterisation of the milled particles

#### 3.1.1. Morphology and microstructure

Ball milling of aluminium in dodecane leads to remarkable changes in the particle morphology (Figure 6, Table 2).

Aluminium is a ductile metal, and therefore upon milling its particles do not undergo cleavage but flattening. As it seen from the SEM images, the initial particles are irregular, mainly elongated and rounded in shape, while the resulting milled particles are fine flakes having rather large lateral sizes (> 10  $\mu$ m) and thicknesses in a range of 50-150 nm. The specific surface area (SSA) of the obtained flake-like particles increases by more than 10 times if it is compared to SSA of the initial powder (Table 2).

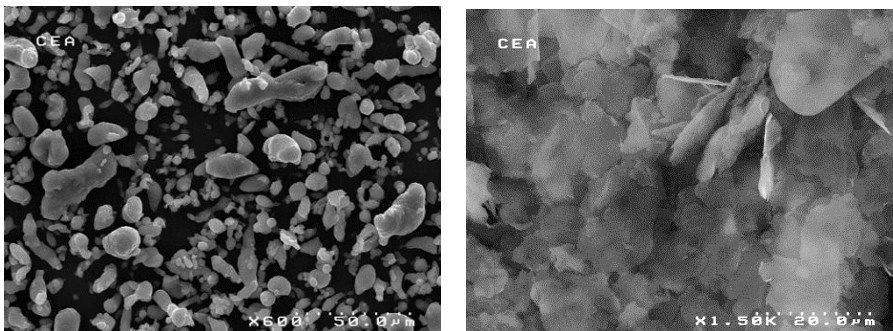


Figure 6 : SEM images of the initial (left) and milled (right) powders of aluminium

Sample	Particle shape	Specific surface area, m <sup>2</sup> /g	particle size from SSA, $\mu$ m	SEM particle size, $\mu$ m
Initial powder	irregular (mainly elongated rounded)	0.56	4.0 <sup>1</sup>	6.1
milled powder	fine flakes	6.33	0.17 <sup>2</sup> (thickness)	0.05-0.20 (thickness)

<sup>1</sup> – particle diameter calculated using (eq.1) ; <sup>2</sup> – particle thickness calculated using (eq.2)

Table 2 : Comparison between aluminium powders before and after ball milling

The obtained SSA values can be used to calculate the particle size. If one assumes the particles to be spherical, the following equation can be applied:

$$d_s = 6 / (SSA \cdot \rho_{Al}) \quad (\text{eq.1})$$

Where  $\rho_{Al}$  is the density of aluminium and  $d_s$  is the particle diameter. The particle size of the initial particles is  $4.0 \mu\text{m}$ , which close to the average size of  $6.1 \mu\text{m}$  determined from the SEM characterisation. In case of flat discoid particles when the particle thickness ( $h$ ) is much smaller than the particle diameter (the case of the milled particles), another equation should be used:

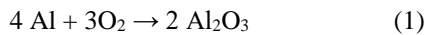
$$h \approx 2 / (SSA \cdot \rho_{Al}) \quad (\text{eq.2})$$

With the help of the equation 2, the average thickness of the milled particles was found to be 117 nm that is good correlation with the SEM observations.

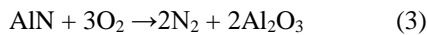
The XRD analysis was used to characterise possible structure changes in the milled aluminium. In the XRD, powder patterns of the particles extracted from the metallized there are only peaks attributable to metallic aluminium, and no aluminium oxide peaks were detected. Although the TG-DSC analysis (see below) proves that the content of aluminium oxide appearing after milling is about 8 wt%, it is known that the oxidation at relatively low temperatures gives rise to  $\gamma\text{-Al}_2\text{O}_3$  occurring in an amorphous state. The peaks of aluminium become wider than one can explain by a decrease of the grain size as well as by a formation of different defects such as dislocations and strain caused by milling.

### 3.1.2. Thermal analysis

The thermal oxidation behaviour during linear heating up to  $1200^\circ\text{C}$  in an air flow was characterised using the TG-DSC analysis (Figure 8, Figure 9) which allows a simultaneous recording of the mass change and the flow of the absorbed heat (endothermal effect) or desorbed heat (exothermal effect) by a sample. The chemical reaction of the aluminium oxidation can be expressed as follows:



According to this reaction, the theoretical mass gain is 89 %. It is assumed that the oxidation in air at temperatures above  $500^\circ\text{C}$  can lead to an intermediate product AlN [10] with the likely reactions as follows:



Since aluminium nitride is supposed to be completely reoxidized at high temperatures (reaction 3), the overall mass gain remains the same. The XRD analysis (see below) of the oxidised product does not show any peaks related to AlN that confirms that even if the reaction 3 occurs, in the end, nitride is fully converted into oxide.

The comparison of the TG-DSC curves (Figure 8, Figure 9) of the initial and milled powders shows interesting results. The mass gain of the non-treated particles reaches only 2 % before the aluminium melting point ( $660^\circ\text{C}$ ). The milled powder shows a greater mass gain (17 %) before the same temperature. This means that before aluminium melting, the oxidation in both cases occurs slowly leading only to a slight increase of the oxide layer on the particle surface.

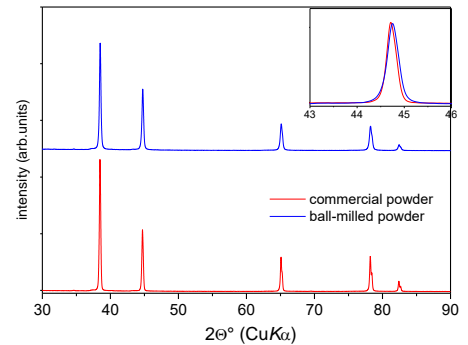


Figure 7 : XRD powder analysis of the initial (red line) and milled (black line) powders. In the inset: zoomed range between  $43$  and  $46^\circ$  ( $2\theta$ ).

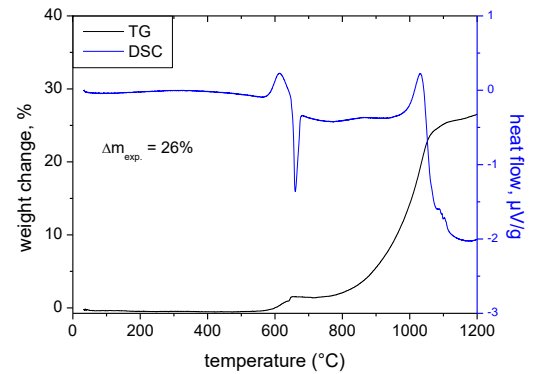


Figure 8 : TG-DSC analysis of the initial aluminium powder

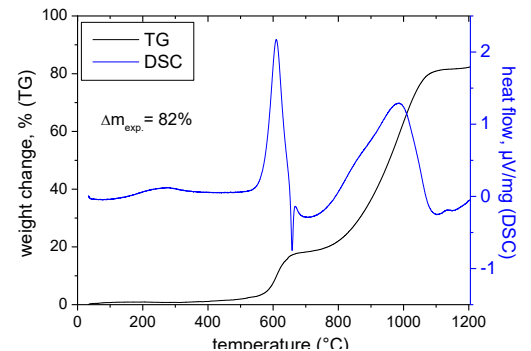


Figure 9 : TG-DSC analysis of the ball-milled aluminium powder

The more important mass gain in the case of the milled particles can be explained by the fact that their surface area is much larger. In both cases, a rapid mass gain starts at temperatures above the melting point of aluminium. According to the oxidation mechanisms of aluminium particles studied earlier [10], the metal melting leads to a rupture of the oxide layer that promotes a better oxygen diffusion inside the particles. As seen from the TG-DSC curves, this process in both cases accelerates at  $T > 800^\circ\text{C}$  and slows down at  $T > 1050^\circ\text{C}$ . After heating up to  $1200^\circ\text{C}$ , the conversion of non-treated particles into oxide reaches only 29.4 % (Table 3).

Analysed powder	$T_{\max}$ , $^\circ\text{C}$	$\Delta m_{\exp}$ (30-660 $^\circ\text{C}$ ), %	$\Delta m_{\exp}$ (30-1200 $^\circ\text{C}$ ), %	Active Metal Content, $C_{AM}$ , %	Conversion coefficient $\alpha$ , % <sup>2</sup>	Ref.
Micrometric powder (Alfa-Aesar)	615	2	26	99.5	29.4	this work
Milled powder	605	17	82	92.3	99.8	this work
Nanopowder (d=150 nm)	580	23	71	85	93.9	[10]
Nanopowder Alex (d ~ 200 nm) <sup>1</sup>	597	26	68	89	85.8	[11]

1 – Particle size calculated from the measurement of specific surface area using (eq. 1)

2 – Conversion coefficient is determined using the equation  $\alpha = \Delta m \cdot 100 \% / (C_{AM} \cdot 0.89)$  [12]

Table 3 : Comparison of the oxidation characteristics of different aluminium powders

This correlates with the previous studies of the oxidation of bulk aluminium. The incomplete metal conversion was confirmed by the XRD analysis of the solid product collected after the TG-DSC analysis. One can see in the XRD pattern (Figure 10) peaks related to metallic aluminium and  $\alpha\text{-Al}_2\text{O}_3$ . The use of the RIR method, which compares the relative XRD peaks intensities of analysed phases and corundum, allowed calculating the content of  $\text{Al}_2\text{O}_3$  in the heated sample.

The

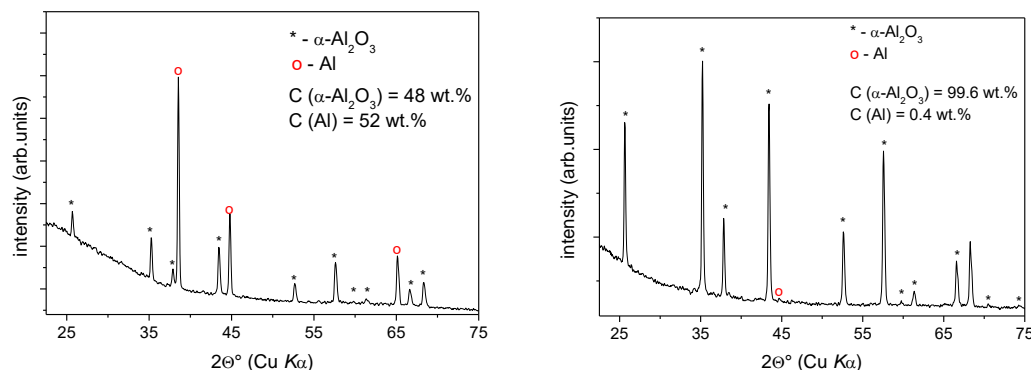


Figure 10: XRD powder analysis of the initial aluminium powder (right) and milled aluminium powder (right) oxidized at  $1200^\circ\text{C}$

obtained value (48 wt %) correlates well with the conversion degree determined from the TG measurement. In fact, the obtained value of 29.4 % of aluminium converted into oxide corresponds to the formation of 44 wt % of  $\text{Al}_2\text{O}_3$  in the sample if one takes into account the difference between the molecular masses of aluminium and its oxide ( $M_w(\text{Al}_2\text{O}_3) = 102 \text{ g/mol}$  and  $M_w(\text{Al}) = 27 \text{ g/mol}$ ). The conversion coefficient of the milled powder is close to 100%. According to the RIR-XRD analysis, the content of the non-oxidised metal in the heated product is only 0.4%. It is noteworthy that this sample shows a higher conversion than aluminium nanopowders studied elsewhere (Table 3) [10] [11]. The content of  $\text{Al}_2\text{O}_3$  in the milled sample before heating is about 8 % that is lower than it is usually observed for nanopowders where the oxide content can reach up to 40%. This result implies that the aluminium obtained by milling yields upon heating a heat combustion which is only 8 % less than the theoretical one.



### 3.2. Characterisation of metallized fuel

The metallized fuel was obtained in one-step by a wet (also called colloidal) ball milling method. Alcoholic solvents and hydrocarbons such as isopropyl alcohol and petroleum spirit are often used for this type of mechanical treatment allowing a smaller particle size and a better particle dispersion. The addition of the surfactant agent is also important as it permits to hinder the metal particle aggregation caused by cold-welding. In our work, we used dodecane as a dispersing liquid and oleic acid as a surfactant. As the final fuel was supposed to be based on this solvent, this allowed a simple, one-step preparation of the desired fuel composition. The ratio between aluminium and dodecane taken for milling was especially chosen to yield a fuel with the target metal concentration of ~20 wt%. Therefore, no further dilution neither concentration was needed. The density of the obtained fuel is close to 875 kg/m<sup>3</sup> at ambient temperature.

The lower heating value (LHV) experimentally determined using an oxygen bomb calorimeter are presented in Table 4. In terms of volumetric LHV (MJ/L), the MF increase by 8.8% in bomb calorimeter. This obtained experimental LHV<sub>v</sub> value is in a good correlation with the theoretical one presented in Table 1 and calculated for a 20 wt% fuel.

Fuel	$\rho_{\text{exp}}$ , kg/L	LHV <sub>m</sub> , MJ/kg	$\Delta$ LHV <sub>m</sub> , %	LHV <sub>v</sub> , MJ/L	$\Delta$ LHV <sub>v</sub> , %
n-dodecane (N-C12)	0.749	44.68±0.32	0	33.47±0.24	0
Metallized fuel (MF)	0.876	41.55±0.41	-7.0±0.7	36.40±0.36	8.8±0.6 %

Table 4 : Experimental density and lower heating values of dodecane and metallized fuel

### 3.3. Stability of metallized fuel

From numerous months to few years may occur between the manufacturing of the metallized fuel and its use. At a lab level, the chosen formula (n-dodecane + 20 wt% aluminium particles) has a useful stability in time. Further studies has to follow to ensure the MF stability in long-term storage with various environments (temperature and pressure cycles, vibrations...).

### 3.4. Viscosity

Metallized Fuel (MF) follows a non-Newtonian dynamic viscosity. In this case, team in [13] reviewed classical semi-empirical viscosity laws. Some of them are presented in Figure 11 for a metallized fuel (MF) with n-C12 and aluminium particles. Those classical theoretical laws widely underestimate rheological measurements [14]. Some semi-empirical laws are based on experiments [14][15], to estimate the dynamic viscosity of metallized fuels, depending on weight fraction of particles for low concentrations (from 0 to 4 wt%).

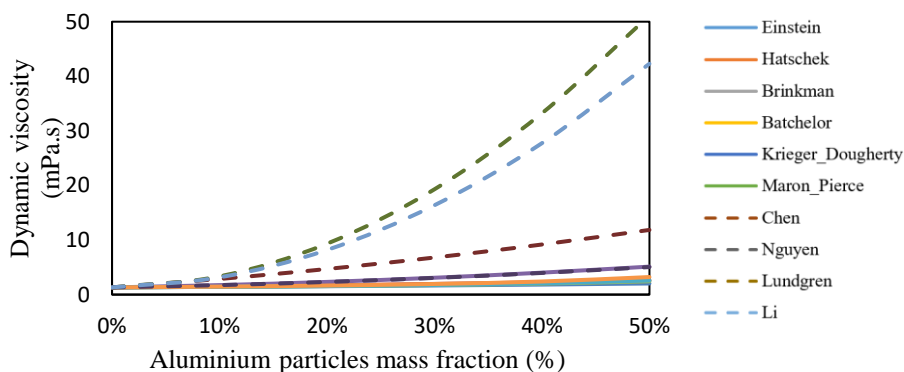


Figure 11 : Dynamic Viscosity Models of Metallized Fuels with respect to mass fraction

Semi-empirical viscosity models are highly dependent on fluid characteristics, temperature, nanoparticles size and nanoparticles shape. Each researcher has its own model; it is therefore difficult to estimate the dynamic viscosity of our nanofluid. For high concentration of aluminium particles in n-dodecane (>25 wt%), values of dynamic viscosity with a semi-empirical model from literature (Nguyen's model, based on experiments) can be 10 times bigger than values from a classical theoretical model (Einstein's model). Metallized fuel studied here contain ~20 wt% of aluminium particles which limit the potential risk of prohibitive dynamic viscosity. Rheological measurements would come to complete this study and identify the most relevant viscosity law in our case.

#### 4. Expected performances

As presented before, a fraction of metallic particles can improve the combustion heating value of fuels. A generic supersonic antiship missile was considered to estimate the potential gain of metallized fuels compared to reference fuel (n-dodecane) in a representative system. A liquid fuel ramjet (LFRJ) propels the missile. Its combustion chamber contains an Integral Booster (IB) to reach Mach 2 and start the ramjet. The missile mass with reference fuel is around 1000kg, with a fixed volume of fuel of 0.243 m<sup>3</sup>. Combustion efficiency and ramjet characteristics are assumed to be the same between n-C12 and MF in this study, as the lab evaluation shows complete combustion for both fuels in ambient initial combustion.

The MF studied here is n-dodecane with 20 wt% aluminium particles (ball-milled as presented in previous section). The theoretical gain (in term of LHV<sub>v</sub>) is near 9% and the theoretical loss (in term of LHV<sub>m</sub>) is near -6%.

Due to the larger mass of metallized fuel, the transition Mach number between IB and LFRJ for the missile with MF is slightly lower than with n-C12. At low altitudes, transition Mach number could be slightly below Mach 2. Computed ignition delay could be lower with metallized fuel (kerosene + aluminium) compared to the fuel itself (if the thin aluminium oxide layer at surface of particles is rapidly fractured) [5]. This effect could allow to ignite the LFRJ at lower speeds. A similar work to [5] could be achieve for our MF compared to n-C12, as detailed kinetic models of n-dodecane are already available.

	Density <sub>exp</sub> (kg/m <sup>3</sup> )	LHV <sub>m</sub> theo (MJ/kg)	LHV <sub>m</sub> exp (MJ/kg)	ΔLHV <sub>m</sub> exp (%)	Fuel mass (kg)	Transition Mach Low altitude
<b>N-Dodecane (N-C12)</b>	749	44.68	44.68±0.32		182	2.00
<b>Metallized fuel (MF)</b>	875	41.94	41.55±0.41	-7.0±0.7%	213	1.97

Table 5: Experimental characteristics and trajectory assumptions for the reference fuel and MF

Two trajectories were considered:

- A simplified trajectory performed by the generic antiship missile is a supersonic cruise (Mach 2) at low altitudes. The missile is fired at Mach 0.9 at sea level.
- A “Medium - High – Low” trajectory (MHL), presented in Figure 12. The firing conditions are Mach 0.8 at an altitude of 5000m

Missile with n-C12 or MF are assumed to be fired in the same conditions and must follow the same trajectory constraints.

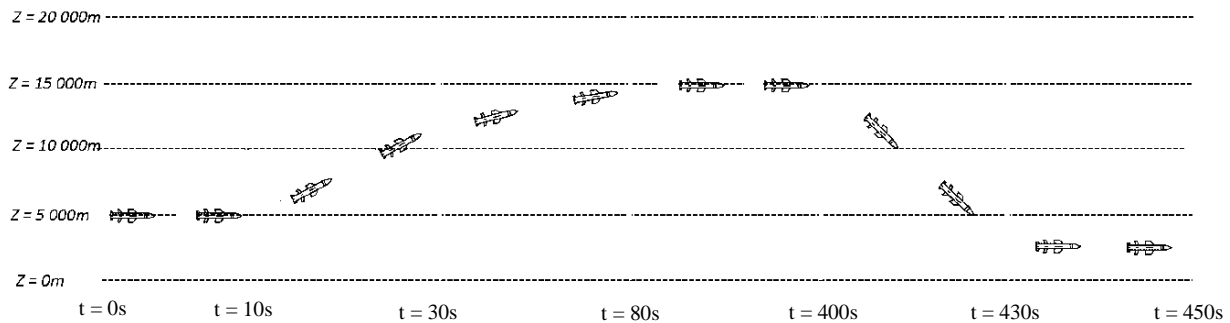


Figure 12: MHL typical trajectory considered in the generic system study



For a supersonic cruise at low altitudes, the range benefit for the missile with MF is near 9%, while the range gain on a “Medium-High-Low” trajectory is close to 11% (Table 6). These values are close from LHV<sub>v</sub> of MF, compared to n-C12 LHV<sub>v</sub>.

	Fuel mass (kg)	$\Delta\text{LHV}_v \text{ exp}$ (%)	$\Delta\text{Range : Sea-Level}$ Mach 2 (%)	$\Delta\text{Range Medium-High-Low}$ (%)
<b>N-Dodecane (n-C12)</b>	182			
<b>Metallized fuel (MF)</b>	213	8.8±0.6 %	8.9%	10.5%

Table 6 : Computed benefits of MF for the two considered trajectories

In terms of performance, MF has an ISP from 5.7% to 6.8% lower than n-C12, depending on flight Mach number (Figure 13 with an altitude of 5000m with an Equivalence Ratio of 0.7)). According to Table 5, the lower heating value by mass (LHV<sub>m</sub>) of MF is 6.9% lower than LHV of n-C12.

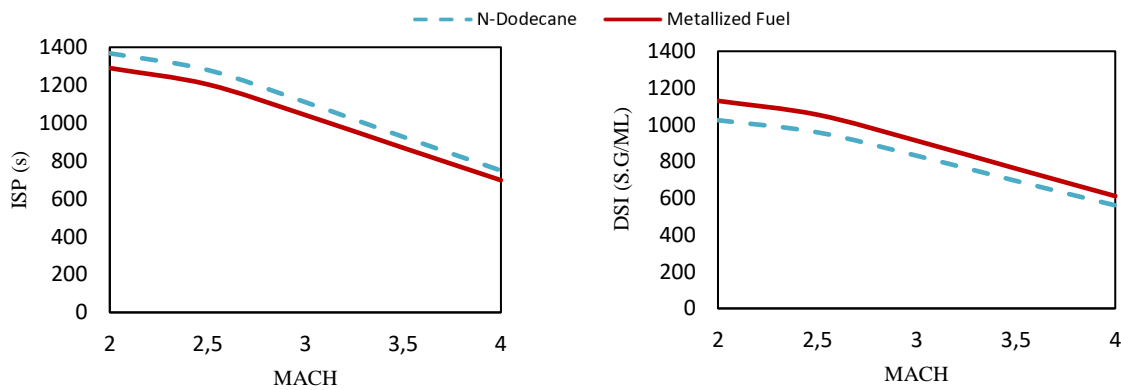


Figure 13 : Computed Specific Impulse of considered ramjet as a function of flight Mach number (fixed Equivalence Ratio = 0.7)

Another useful metric is the Density Specific Impulse (DSI), which is  $\text{ISP} \times \text{Density}$  in s.g/mL. This value represents the energetic density of a given volume of fuel. Therefore, the comparison between the gain of Lower Heating Value by volume (LHV<sub>v</sub>) and DSI looks attractive. Table 7 shows the same order of magnitude of gain between DSI and LHV<sub>v</sub>, which confirms the consistency between LHV gains and concrete performance benefit between n-C12 and MF with an affordable technology.

	Density (kg/m <sup>3</sup> )	$\Delta\text{LHV}_{m\text{exp}}$ (%)	$\Delta\text{ISP}$ (%)	$\Delta\text{LHV}_{v\text{exp}}$ (%)	$\Delta\text{DSI}$ (%)
<b>N-Dodecane (n-C12)</b>	749				
<b>Metallized fuel (MF)</b>	875	-7.0±0.7%	-6.3±0.6%	8.8±0.6 %	9.6±0.7 %

Table 7 : Comparison between experimental energetic values and computed specific impulse

## 5. Conclusion:

The potential of affordable metallized fuel was investigated both at lab scale and with generic system analysis of ramjet powered antiship missile. The stability and performance of a generic metallized fuel based on 20 wt% of aluminium nanoscale particles in n-dodecane were demonstrated. Further activities shall include rheology characterization as well as kinetic modelling.

## Acknowledgments:

The authors would like to thank all the colleagues that participate in some extend to the current study reported here, especially Sandra, Bernard, Constantin, Tiphaine ...

## 6. References

- [1] Ben Said L., Ghachem K. et al. (2022). Advancement of nanofluids in automotive applications during last few years - a comprehensive review. *Journal of Thermal Analysis and Calorimetry*
- [2] Ojha P.K., Karmakar S. et al. (2018). Boron for liquid fuel Engines-A review on synthesis, dispersion stability in liquid fuel, and combustion aspects. *Progress in Aerospace Sciences*
- [3] Anbarsooz M. (2022). Combustion characteristics of nanofuels : A comprehensive review on diesel/biodiesel-based nanofuels. *Fuel*
- [4] Boyet G., Cochet A. et al. (2001). Statoréacteur à combustible dense au Bore : maitrise technologique et potentialités opérationnelles. *Colloque commun Aérodynamique et Propulsion, AAAF Arcachon*
- [5] Chatelain K.P., Matra M. et al. (2019). Development of Kinetic Models for the Hybrid Fuels Combustion Containing Aluminium Particles. *Journal of Propulsion and Power*
- [6] Luo Y., Xu X. et al. (2016). Combustion of JP-10-Based Slurry with Nanosized. *Journal of propulsion and power*
- [7] Jin Y., Yang Q. et al. (2021). Performance characteristics of a scramjet engine using JP-10 fuel containing aluminium nanoparticles. *Acta Astronautica*
- [8] Jin Y., Xu X. et al. (2022). Propulsive and combustion behavior of hydrocarbon fuels containing boron nanoparticles in a liquid rocket combustor. *Journal of aerospace engineering*
- [9] Corporan E., Williams V. et al. (2022). High temperature fuel impacts on combustion characteristics of a swirl-stabilized combustor. *Fuel*
- [10] Noor F., Zhang H. et al. (2013). Oxidation and ignition of aluminium nanomaterials. *Physical Chemistry Chemical Physics*
- [11] Kwon Y.S., Gromov A. et al. (2007). Passivation of the surface of aluminium nanopowders by protective coatings of the different chemical origin. *Applied Surface Science*
- [12] Korotkikh A.G., Sorokin I.V. (2019). Study of the chemical activity of metal powders based on aluminium, boron and titanium. *AIP Conference Proceedings*
- [13] Murshed S.M., Estellé P. (2017). A state of the art review on viscosity of nanofluids. *Renewable and Sustainable Energy Reviews*
- [14] Sundar L.S., Sharma K.V. et al. (2013). Empirical and theoretical correlations on viscosity of nanofluids : A review. *Renewable and Sustainable Energy Review*
- [15] Li S., Yang Q. et al. (2022). Effect of Nanoparticle Concentration on Physical and Heat-Transfer Properties and Evaporation Characteristics of Graphite/n-Decane Nanofluid Fuels. *ACS Omega*